The static and dynamic critical behaviour of the two-dimensional Heisenberg antiferromagnet $KFeF_4$

1994 J. Phys.: Condens. Matter 6 6679

(http://iopscience.iop.org/0953-8984/6/33/015)

J. Phys.: Condens. Matter 6 (1994) 6679–6690. Printed in the UK

The static and dynamic critical behaviour of the two-dimensional Heisenberg antiferromagnet $KFeF_4$

S Fulton†, R A Cowley†, A Desert‡ and T Mason§¶

† Clarendon Laboratory, Oxford University, Oxford, UK

‡ Laboratoire de Physique de L'Etat Condensé, Université du Maine, France

§ Risø National Laboratory, Roskilde, Denmark

Received 9 May 1994, in final form 10 June 1994

Abstract. $KFeF_4$ is a well characterized planar antiferromagnet with $S = \frac{5}{2}$, and is an excellent example of a two-dimensional Heisenberg antiferromagnet. Using neutron-scattering techniques, a study of both the static and dynamic critical behaviour above the Néel temperature, $T_N = 136.75 \pm 0.35$ K, has been undertaken. It is found that in the region above $1.04T_N$, the static correlation length, the structure-factor peak intensity and the width of the dynamic scattering are all qualitatively described by the theories developed for Heisenberg antiferromagnets. The data have been compared with both the theory for a quantum Heisenberg antiferromagnet, as developed for La_2CuO_4, and also the model for a classical Heisenberg antiferromagnet. Both these theories describe the data equally well. Below $1.04T_N$ the system is expected to behave like a two-dimensional Ising system.

1. Introduction

With the discovery of the cuprate superconductors [1] has come a renewed interest in two-dimensional antiferromagnets [2]. In the undoped phase these cuprates are not superconducting but are found to order antiferromagnetically [3] and it is believed that the magnetism plays an important part in the processes that lead to the superconducting state [4]. This new impetus has renewed interest in the theory of the critical behaviour of two-dimensional systems, and descriptions have now been developed for the two-dimensional quantum Heisenberg antiferromagnet (QHAF) [5]. This theory is a renormalization of the classical lattice rotator model (CLRM) [6] and has been successfully used to describe the $S = \frac{1}{2}$ QHAF La_2CuO_4 [5] and the $S = 1$ system K_2NiF_4 [7].

Many experiments were performed on the two-dimensional antiferromagnets with the K_2NiF_4 structure in the 1970s [8, 9]. In these systems the low-temperature behaviour is dominated by small Ising-like anisotropy terms, leading to two-dimensional Ising critical behaviour below T_N. For K_2NiF_4 it is found that the Ising behaviour persists above T_N until a crossover to a Heisenberg region is reached. Birgeneau and co-workers fitted the static correlation length of K_2NiF_4 to the two-dimensional Ising model between T_N and $1.05T_N$ [8], and above this showed [7] that the system gives excellent agreement with the two-dimensional isotropic QHAF theory developed by Chakravarty, Halperin, and Nelson (CHN) [5].

$KFeF_4$ [10, 11] is similar in many ways to the K_2NiF_4 systems. Like these materials it has magnetic planes separated from each other by sheets of non-magnetic ions, leading to

¶ Present address: Department of Physics, University of Toronto, Toronto, Ontario, Canada M5S 1A7.

0953-8984/94/336679+12$19.50

weak interplanar interactions. In $KFeF_4$ this leads to a ratio of the order of 10^{-4} between interplanar and intraplanar interactions. It also has a weak Ising-like anisotropy term, which aligns the spins along the crystallographic *c*-axis. This term dominates the critical behaviour below T_N. Previous work [19] has shown that the staggered magnetization has a power-law temperature dependence with $\beta = 0, .130 \pm 0.005$ [11], close to the theoretical prediction for a two-dimensional Ising system [12].

The nature and strength of the interactions were determined by measuring the spin-wave dispersion curves [19, 11], and the purpose of this work is to study how these interactions affect the magnetic critical behaviour (both static and dynamic) of $KFeF_4$ above T_N. A single crystal of $KFeF_4$ was studied with inelastic-neutron-scattering techniques. The results from this experiment have been compared to the theory for both a two-dimensional Ising system and the models for a Heisenberg antiferromagnet in order to study the crossover behaviour.

The next part of this paper is a summary of the theoretical results for the two-dimensional Heisenberg and the two-dimensional Ising models. Following this, there is a discussion of the experimental arrangement and the analysis of the data. Finally we present a comparison of the results extracted from the data with the theories.

2. Theory

Two-dimensional Heisenberg antiferromagnets have no long-range order (LRO) above $T = 0$ K. It is the weak anisotropies or interplanar interactions in real systems that lead to LRO at finite temperatures. In the theories described below, it is assumed that the ground state with conventional antiferromagnetic order occurs only at $T = 0$ K and the correlation functions for the LRO decay are described from this point rather than from a finite Néel temperature as in real systems.

The CLRM [6] predicts that the correlation length in a classical Heisenberg antiferromagnet is given by

$$\xi/a_{NN} = B_\xi \exp(2\pi\rho/k_B T)/(2\pi\rho/k_B T + 1) \tag{1}$$

where $B_\xi = 0.01$, a_{NN} is the nearest-neighbour separation, and ρ is the classical value of the spin-wave stiffness constant without the spin fluctuation terms (see equation (3) below).

CHN have taken the classical model for a two-dimensional Heisenberg antiferromagnet and have renormalized the results to take into account quantum fluctuations, and introduced the thermal de Broglie wavelength, $\hbar c/k_B T$, as a short-wavelength cut-off instead of a constant multiplied by the lattice spacing a_{NN}, which is used as a length scale in the classical problem. Using this method they have produced a model for the QHAF to describe the instantaneous correlations, which gives reasonable agreement with the available experimental data [5, 7].

The CHN theory predicts that the correlation length is given by

$$\xi/a_{NN} = C_\xi \exp(2\pi\rho/k_B T)/(1 + k_B T/2\pi\rho). \tag{2}$$

Notice the difference in the denominators in equations (1) and (2); this difference arises from using the thermal cut-off instead of a constant multiplied by the lattice spacing. In

equation (2), ρ is the spin-wave stiffness constant defined such that

$$2\pi\rho = 2\pi J_{NN} S^2 Z_c(S)^2 Z_x(S) \tag{3}$$

$$Z_c = 1 + 0.158/2S + O(1/2S)^2 \tag{4}$$

$$Z_x = 1 - 0.552/2S + O(1/2S)^2 \tag{5}$$

with J_{NN} being the nearest-neighbour exchange constant and S the spin. The Z_c and Z_x terms are correction factors to take account of the quantum fluctuations. For $KFeF_4$, $S = \frac{5}{2}$ and J_{NN} has been taken as the average of the nearest-neighbour in-plane exchange constant, 2.445 meV. The correction terms change the spin-wave stiffness constant by 5% from its classical value for $S = \frac{5}{2}$ systems, while for $S = \frac{1}{2}$ systems the quantum fluctuations are much more important and the spin-wave stiffness constant is changed by 40%.

CHN predict that the constant C_ξ has the following form:

$$C_\xi = \sqrt{32}e^{\pi/2} B_\xi / C_\rho \tag{6}$$

with

$$C_\rho = 2\pi S Z_x Z_c / \sqrt{8} \tag{7}$$

which gives $C_\xi \simeq 0.06$ to within 30% for $S = \frac{1}{2}$. This is almost twice as large as the value predicted by Manousakis and Salvador [13] using Monte Carlo simulations. The uncertainty in the CHN theory arises from the uncertainty in B_ξ, the value calculated for the classical-model scaling factor. Hasenfratz and Niedemayer [14] have predicted that the prefactor is

$$C_\xi = e/8C_\rho. \tag{8}$$

This gives $C_\xi \simeq 0.07$ for $S = \frac{5}{2}$. It is clear from this discussion that the scaling constant, C_ξ, is not a well known parameter.

The structure factor for both the CLRM and the QHAF models depends upon the correlation length in the following way:

$$S(0) = C_s \xi^2 / \left[\left(2\pi\rho/k_B T\right) + 1\right]^2 \tag{9}$$

where C_s is another constant.

Equations (1)–(9) then fully describe the static correlation function for both the CLRM and the QHAF models.

The dynamic response of the two-dimensional Heisenberg system has been studied by Tyc *et al* [15]. The frequency width of the correlation function $S(k, \omega)$, at $k = 0$, is given by

$$\Gamma = \gamma\bar{\omega}_0 = \gamma c \xi^{-1} (T/2\pi\rho)^{1/2} \tag{10}$$

where, if c is the spin-wave velocity in millielectronvolt ångstroms, and Γ is in units of millielectronvolts, $\gamma \simeq 0.85 \pm 0.15$ [16]. For $KFeF_4$ c is obtained from the dispersion curves [11] as $c = 70$ meV Å.

The data were also fitted to the power laws such as characterize the temperature dependence close to T_N when $T_N \neq 0$. For example, the correlation length was fitted to

$$\xi/a_{NN} = 1/\kappa a_{NN} = K_0 t^{-\nu}. \tag{11}$$

Here κ is known as the inverse correlation length. For a two-dimensional Ising system $\nu = 1$ and K_0 is a scaling constant, which for a two-dimensional square lattice has the value 1.763 [17].

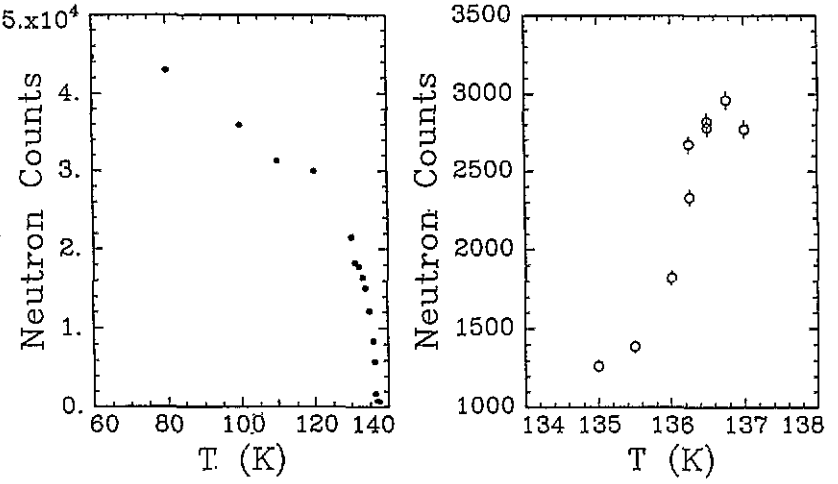

Figure 1. The temperature dependence of the (1, 1, 0) magnetic Bragg peak, which measures the extent of the three-dimensional ordering, is shown on the left-hand side and the temperature dependence of the scattering for a wavevector transfer (1, ,1, 0.53), which is proportional to the static susceptibility, on the right.

3. The sample and experimental preliminaries

The $KFeF_4$ single crystal was grown at the Université du Maine using the Bridgman Stockbarger technique in a platinum crucible. The crystal was a small plate $4 \times 3 \times 15$ mm^3. This crystal was used in a previous neutron-scattering study [10]. In the (h, h, l) scattering plane the mosaic spread is 0.09°. At room temperature $KFeF_4$ has an orthorhombic structure, with $a = 7.81$ Å, $b = 7.64$ Å, $c = 12.40$ Å.

From our low-temperature studies (on a different sample) we found that the average of the exchange interactions in the a and b directions was $J_{NN} = 2.455$ meV, where the Hamiltonian is of the form

$$H = \sum_i g\mu_B H_A S_i^Z + \sum_{ij} J_{ij} \boldsymbol{S}_i \cdot \boldsymbol{S}_j \tag{12}$$

and $g\mu_B H_A = 0.12$ meV is the anisotropy energy, which tends to align the spins along the crystallographic c-axis.

The crystal was mounted with the (h, h, l) plane as the scattering plane and was placed in a variable-temperature, closed-cycle cryostat so that the temperature could be varied.

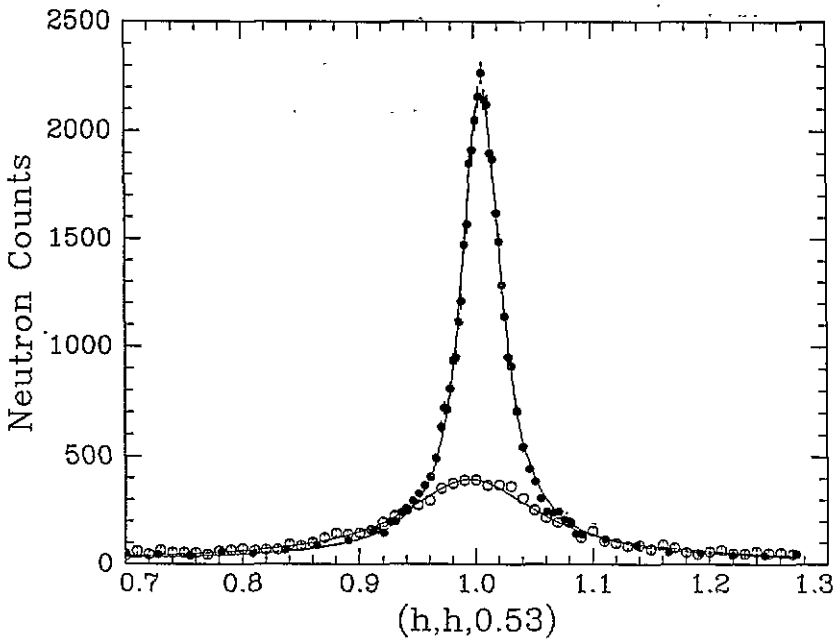

Figure 2. The critical scattering intensity at 147 K (filled circles) and 180 K (open circles).

The neutron scattering was studied using the TAS6 instrument at the Risø facility in the two-axis mode, the energy analyser having been removed in order that the energy integrated intensity could be measured. A pyrolytic-graphite monochromator was used to produce a monochromatic beam of neutrons with a wavevector of 2.51 $Å^{-1}$, and a pyrolytic-graphite filter was placed between the monochromator and sample to suppress higher-order neutrons. The collimation used was 30′ before the monochromator, 36′ between the monochromator and sample and 22′ between the sample and detector. The resolution function was measured using the (110) magnetic Bragg reflection and was found to have a width (FWHM) along $(\zeta, \zeta, 0)$ of 0.027 $Å^{-1}$ and vertically of 0.113 $Å^{-1}$.

The transition temperature, T_N, of $KFeF_4$ was determined by measuring the temperature dependence of the $(1, 1, 0)$ magnetic Bragg peak, which measures the extent of the three-dimensional ordering, and from the temperature dependence of the scattering observed with a wavevector transfer of $(1, 1, 0.53)$, which is a measure of the two-dimensional susceptibility. The results are shown in figure 1 and give a transition temperature $T_N = 136.75 \pm 0.25$ K, in good agreement with previous studies of $KFeF_4$ [17, 18].

The static critical scattering was then measured by scanning the wavevector transfer along the line $(\zeta, \zeta, 0.53)$ in reciprocal space. This point was chosen so that the scattered wavevector was parallel to the c-axis so that the scattering is only slowly varying, and the two-axis experiment integrates over the energy dependence of the critical scattering, while keeping the in-plane wavevector transfer constant.

The dynamic scattering was measured using the TAS6 spectrometer in the three-axis mode by placing a pyrolytic-graphite analyser between the sample and detector. The energy resolution was obtained by using a vanadium sample and was found to be 1.012 meV (FWHM). The scans to measure the frequency dependence of the correlation function were taken with Q fixed at $(1, 1, 0.53)$. This point was chosen as it was far away from the Bragg peaks and thus structural effects can be neglected when analysing the data, and also because there should be no contamination from $\lambda/2$ scattering.

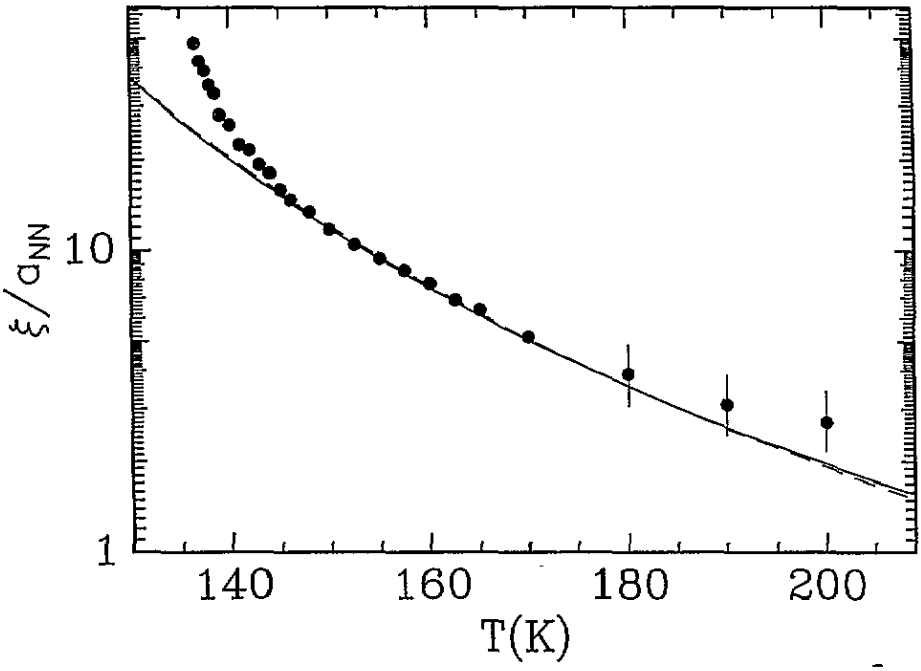

Figure 3. The variation of the static correlation length with temperature. The solid line represents a fit to the CLRM, the dashed to the QHAF model.

A preliminary study of the dynamic scattering had previously been carried out at the ILL on the IN3 instrument. The experimental arrangement was similar to that described in [11] and [19]. In these experiments the crystal was lined up with the *ab*-plane as the scattering plane, and the energy scans were performed with Q fixed at $(1, 1, 0)$. This caused problems as there was a weak structural Bragg peak present, which made it difficult to analyse the data above 170 K. A comparison of the results extracted from the two sets of data will be made in section 5.

4. Experimental results and analysis

The static critical scattering was measured at 27 temperatures between T_N and 240 K. As was expected, qualitatively the results show a decreasing intensity and an increasing width in wavevector as the temperature increases (see figure 2). For a Heisenberg system we expect the susceptibility to be isotropic, i.e. the susceptibility parallel and perpendicular to the spin

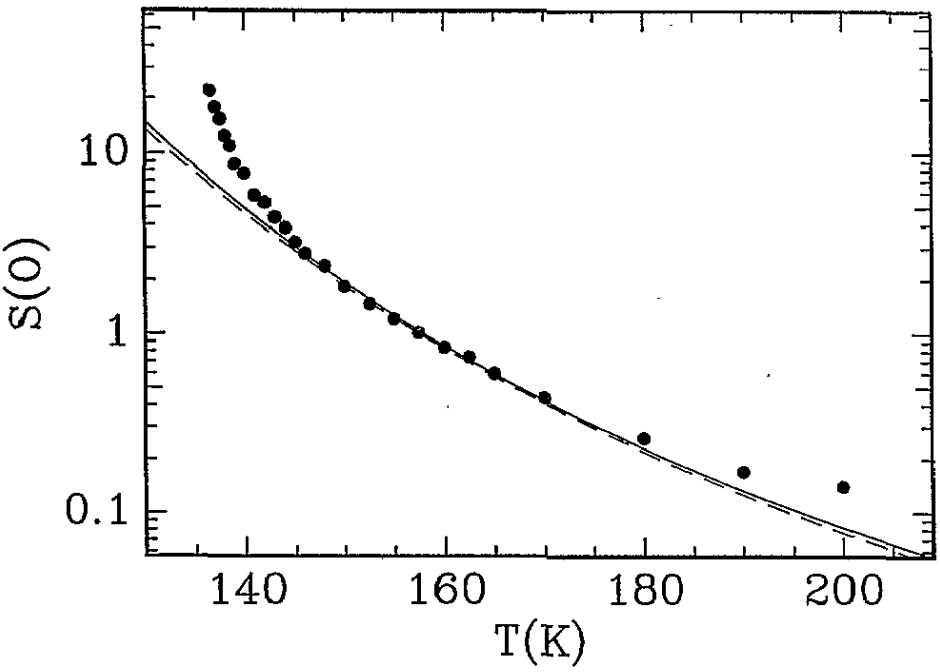

Figure 4. The structure factor as a function of temperature compared with the CLRM model (the solid line) and with the QHAF model (the dashed line).

direction to be the same. For an Ising system the parallel and perpendicular susceptibilities are different, with only the susceptibility parallel to the spin direction becoming critical at T_N. When modelling the susceptibility we have taken the differences between the Heisenberg and the Ising-like systems into account.

The data were analysed by assuming $KFeF_4$ is behaving like an isotropic Heisenberg system and a single Lorentzian was used to describe the scattering:

$$S(q) = A/\left(q_x^2 + q_y^2 + \xi^{-1}\right). \tag{13}$$

This was convolved with a triangular vertical resolution function and with a Gaussian form along the $(\zeta, \zeta, 0)$ direction. In addition the background was held fixed at 18 counts for a monitor 50 000 (this corresponds to approximately 25 s). The results from these fits have been compared to the theories for the two-dimensional Heisenberg model and are shown in figures 3 and 4. The data for both the correlation length, ξ, and for the structure factor, $S(0) = A\xi^{-2}$, are well described by the theories in the region $1.04T_N < T < 1.4T_N$. In the fits, the spin-wave stiffness was held constant as determined in [19] and only the scaling prefactor was allowed to vary. A comparison of the prefactors obtained from the fits with the theoretical predictions will be given in the next section.

The data were also analysed in terms of the Ising model in which the separate contributions from the parallel and perpendicular susceptibilities were taken into account as described in detail in [8]. The data near T_N were fitted to a two-Lorentzian model

$$S(q) = A_{\parallel}/\left(q_x^2 + q_y^2 + \xi_{\parallel}^{-2}\right) + A_{\perp}/\left(q_x^2 + q_y^2 + \xi_{\perp}^{-2}\right). \tag{14}$$

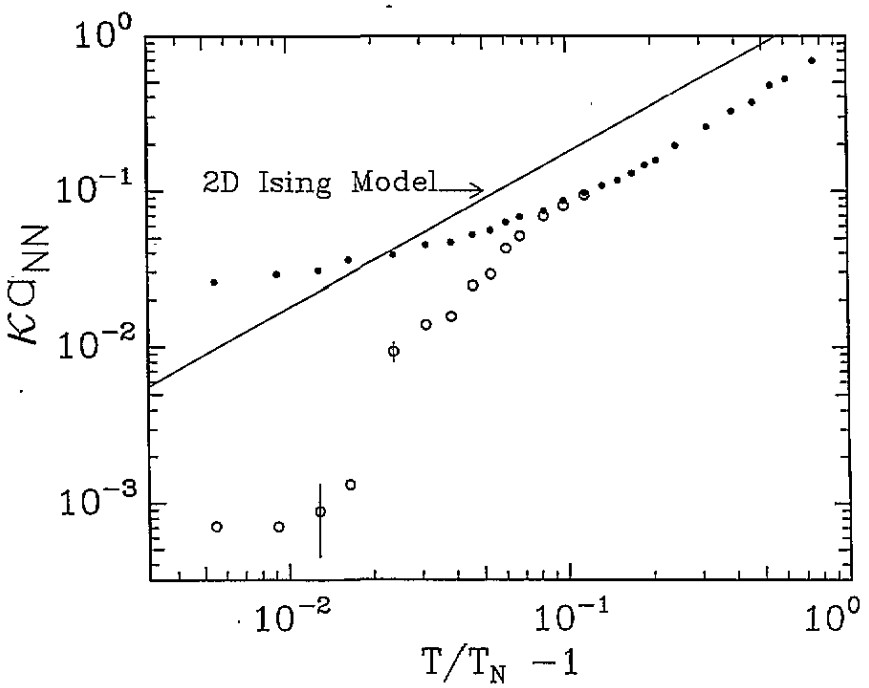

Figure 5. A comparison of the inverse correlation length with the two-dimensional Ising model. The filled circles are data extracted from fits to the Heisenberg model for the susceptibility (equation (13)), while the open circles are fits to an Ising model for the susceptibility (equation (14)). The solid line shows the slope expected for a $d = 2$ Ising system.

For temperatures below $0.95T_N$, the experimental data were fitted to a single transverse Lorentzian and it was found that as the temperature T approached T_N, $A_\perp$ and $\xi_\perp$ became constant, and these constant values were taken to describe the perpendicular susceptibility at T_N; the inverse correlation range $\xi_\perp^{-1}a^*$ was 0.04. The longitudinal susceptibility above T_N was then obtained by extrapolating the form for the transverse susceptibility above T_N and fitting $A_\parallel$ and $\xi_\parallel$ in equation (14) to the data. The extrapolation was performed in two ways. In both cases $A_\perp$ was held constant, but in one case $\xi_\perp$ was held fixed at its value at T_N and in the other case $\xi_\perp$ was assumed to vary with the Ising exponent, $\nu = 1$, but with a transition temperature reduced below T_N by ΔT_N. ΔT_N was taken to be 12 K based on the parameters at T_N. Both approaches gave very similar results for $A_\parallel$ and $\xi_\parallel$ and those of the latter approach are shown in figure 5 along with a comparison to the theory for the two-dimensional Ising model. The two sets of data points represent the fits from both the single- (equation (13)) and two-Lorentzian (equation (14)) models. The analysis for the two-component Lorentzian model fails close to T_N due to the narrow width in reciprocal space of the susceptibility peak. The resolution function and the non-critical perpendicular component make an accurate measurement of the parallel contribution very difficult. The straight line represents a simulation of the two-dimensional Ising model, which we would expect to give a good description of the data asymptotically close to T_N. As is seen, this is clearly not the case. This is different from the results for K_2NiF_4 [8], when a similar analysis was used.

Measurements of the dynamic critical scattering were made at twelve temperatures above T_N and the data were fitted to a single Lorentzian

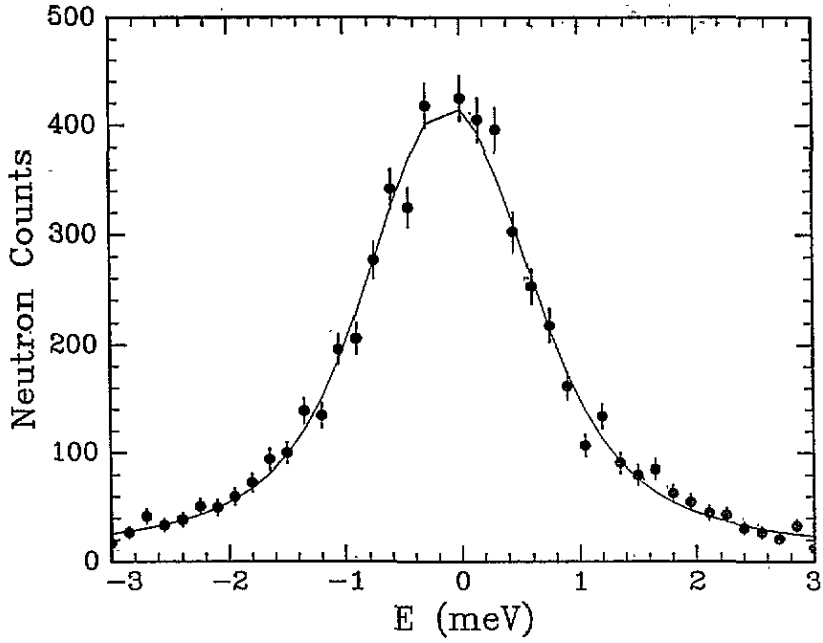

Figure 6. The neutron scattering as a function of energy at 147 K, and a fit to Lorentzian line shape.

$$S(\omega) = A/\left(\omega^2 + \Gamma^2\right) \tag{15}$$

convolved with the energy resolution (see figure 6). The results of these fits for Γ are shown in figure 7 along with the theory for the two-dimensional Heisenberg systems. The data points at 170 K and above are clearly inconsistent with the other data points and the theory. This is possibly due to a breakdown of the analysis procedure as the magnetic contribution is then small. A similar divergence from the theory was also seen in the correlation length and structure factor data at high temperatures, although this occurred at 190 K. The two-dimensional Heisenberg theory for the dynamic scattering has been fitted between 144 K and 160 K by adjusting the scaling prefactor to fit the data. Similar data were also collected at the ILL and the results of the fits to these data are shown in tables 1 and 2.

Table 1. A comparison of the fits to the QHAF model with the theory.

Parameters deduced from	C_ξ	$2\pi\rho/K$	χ^2
ξ	0.010±0.001	1080	4
TAS6:Γ	0.0079±0.0001	1080	1.05
ILL:Γ	0.0080±0.0002	1030	5.5
CHN [5]	0.06	1080	
MS [13]	0.03	1080	

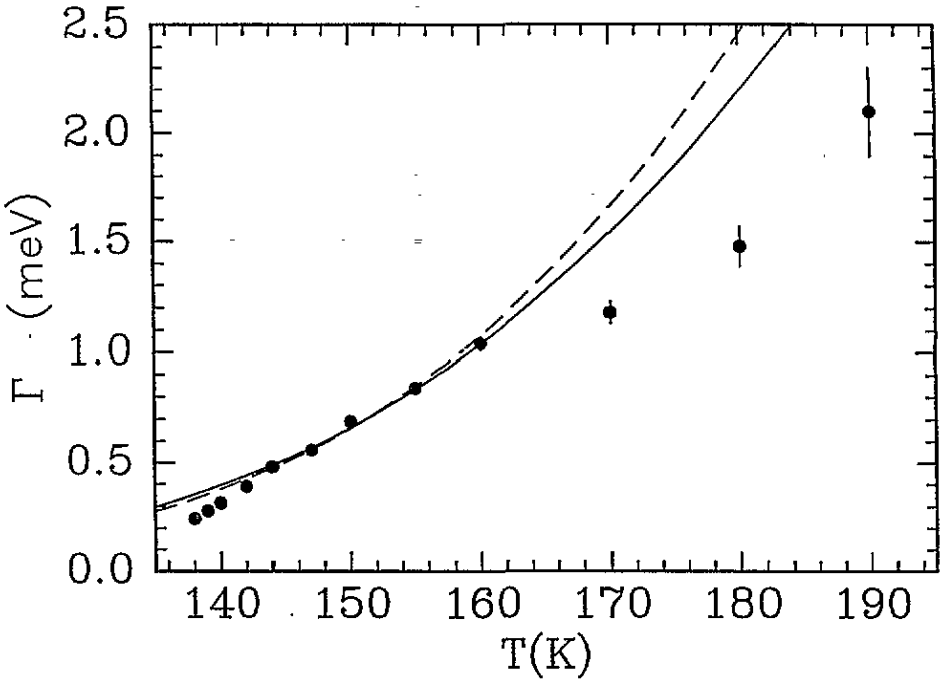

Figure 7. A comparison of the widths from the inelastic scattering, with the predictions of the CLRM (solid line) and the QHAF model (dashed line).

Table 2. A comparison of the fits to the CLRM with the theory.

Parameters deduced from	B_ξ	$2\pi\rho/K$	χ^2
ξ	0.052±0.001	1140	6
ξ	0.033±0.003	1220±15	4
TAS6:Γ	0.039±0.001	1140	0.8
ILL:Γ	0.036±0.001	1090	6.5
CLRM [6]	0.01	1140	

5. A comparison of the experiment with theory

The results of fitting the different experimental results for $KFeF_4$ to the CLRM and the QHAF model are shown in tables 1 and 2 together with the theoretical predictions of CHN [5] and MS [13]. For both theories the scaling constants are approximately fourfold different from the theoretical values. For the QHAF model, the average value of C_ξ is 0.009±0.001. This is three to six times smaller than the theoretical predictions [5, 13] of 0.03–0.06. It was, however, possible to fit the data for $KFeF_4$ to the QHAF model in the region $1.04 < T/T_N < 1.4$ provided that C_ξ was allowed to vary in agreement with the K_2NiF_4 data.

The fits to the CLRM give an average value of $B_\xi = 0.040 \pm 0.010$. This is four times larger than the theoretical value of B_ξ calculated for the CLRM. This model also fitted the data in the temperature region $1.04T_N < T < 1.4T_N$. Both sets of fits (i.e. to the CLRM and the QHAF model) used values of the spin-wave stiffness constant as predicted from the dispersion curves and fitted the data equally well.

Good agreement with the QHAF theory was obtained for the results from K_2NiF_4 [7] in the region $1.05T_N < T < 1.5T_N$. The scaling prefactor for the correlation length obtained from the analysis was within 30% of the CHN theoretical prediction for C_ξ for an $S = 1$ system. Similar analyses for La_2CuO_4 did not give such good agreement with the theory; C_ξ was twice that predicted by CHN for an $S = \frac{1}{2}$ antiferromagnet. The results of fitting the QHAF model to the $KFeF_4$ data are not in such good agreement with the theoretical predictions as these experiments. The scaling factors are of the correct order of magnitude and show that qualitatively $KFeF_4$ agrees with a two-dimensional Heisenberg model in the same temperature range as previous experiments. Since the values deduced for C_ξ are smaller than the predicted values while those for B_ξ are larger, one possibility is that the appropriate model for $KFeF_4$ is intermediate between the CLRM and the QHAF model.

The previous study [19, 11] of $KFeF_4$ showed that below T_N it exhibited two-dimensional Ising-like behaviour. Since with these data it has not been possible to fit to a power-law behaviour in the critical region above the transition temperature (see figure 5), we do not know exactly where the crossover from Ising-like to Heisenberg-like behaviour occurs. Theoretically the crossover occurs [7] when $h_A(\xi/a)^2 \sim 1$. h_A is the ratio of the anisotropy energy to the nearest-neighbour exchange interactions and for $KFeF_4$ $h_A = 0.005$, implying $\xi/a \sim 14$ at the crossover. From figure 3 it may be seen that $\xi/a = 14$ when $T = 143$ K and indeed the theory for the two-dimensional Heisenberg models could not explain the data below this temperature. Note that in the region between T_N and 143 K we were again unable to fit the data to power-law behaviour.

6. Conclusions

Above T_N it has not been possible to fit the static correlation length of $KFeF_4$ to the theory for a two-dimensional Ising model asymptotically close to T_N as was done for K_2NiF_4 and as would be expected from theory. Above $1.04T_N$, $KFeF_4$ seems to be in qualitative agreement with the theories for a two-dimensional Heisenberg system, although the prefactors are not in as close agreement with the theory as for the analyses of the other systems. The analysis seems to break down above $1.4T_N$. To study the crossover from two-dimensional Ising to two-dimensional Heisenberg behaviour it would be necessary to carry out an experiment with better resolution close to T_N.

Acknowledgments

This work was supported by the Science and Engineering Research Council of Oxford, and in Risø by the Large Installation Programme of the European Commission. Sharon Fulton is grateful to the SERC for the award of a studentship.

References

[1] Bednorz J G and Müller K A 1986 *Z. Phys.* B **64** 189
[2] Manousakis E 1991 *Rev. Mod. Phys.* **63** 1
[3] Endoh Y, Yamada K, Birgeneau R J, Gabbe D R, Jenssen H P, Kastner M A, Peters C J, Picone P J, Thurston T R, Tranquanda J M, Shirane G, Hidaka Y, Oda M, Enomoto Y, Suzuki M and Murakami T 1988 *Phys. Rev.* B **37** 7443 and references therein
[4] Anderson P W 1987 *Science* **235** 1196

[5] Chakravarty S, Halperin B I and Nelson D R 1992 *Phys. Rev.* B **39** 2344
Halperin B I 1992 *J. Magn. Magn. Mater.* **104–107** 761
[6] Shenker S H and Tobochnik J 1980 *Phys. Rev.* B **9** 4462
[7] Birgeneau R J 1990 *Phys. Rev.* B **41** 2514
[8] Birgeneau R J, Als-Nielsen J and Shirane G 1977 *Phys. Rev.* B **16** 280
[9] Cowley R A, Shirane G, Birgeneau R J and Guggenheim H J 1977 *Phys. Rev.* B **15** 4292
Birgeneau R J, Guggenheim H J and Shirane G 1973 *Phys. Rev.* B **8** 304
Birgeneau R J, Skalyo J and Shirane G 1971 *Phys. Rev.* B **3** 1736
[10] Desert A, Bulou A and Nouet J 1992 *Solid State Commun.* **83** 505
[11] Fulton S, Nagler S E, Cowley R A and Needham L M 1992 *Physica* B **180 & 181** 225
[12] Collins M F 1989 *Magnetic Critical Scattering* (Oxford: Oxford University Press)
[13] Manousakis E and Salvador R 1988 *Phys. Rev. Lett.* **60** 840; 1989 *Phys. Rev. Lett.* **61** 1310
[14] Hasenfratz P and Niedermayer F 1991 *Phys. Lett.* **268B** 231
[15] Tyc S and Halperin B I 1990 *Phys. Rev.* B **42** 2096
Tyc S, Halperin B I and Chakravarty S 1989 *Phys. Rev.* B **62** 835
[16] Halperin B I *J. Magn. Magn. Mater.* **104–107** 761
[17] Eibshutz M, Davidson G R, Guggenheim H J and Cox D E 1972 *AIP Conf. Proc.* **5** 670
[18] Keller H and Savic I M 1983 *Phys. Rev.* B **28** 2628
[19] Fulton S, Nagler S E, Needham L M and Wanklyn B M 1994 *J. Phys.: Condens. Matter* **6** 6667–78